Evaluation of Stability and Geotechnical Performance of *Hopper* Retaining Walls Using PLAXIS 2D (*Hardening Soil Model*)

Muhammad Shohib[1*] , Hanie Teki Tjendani[2] , Jaka Purnama[3]

[1,2,3] Program Studi Magister Teknik Sipil, Fakultas Teknik, Universitas 17 Agustus 1945 Surabaya
* Corresponding author. Email: muhammadshohib911@gmail.com

ABSTRACT

This study aims to evaluate the geotechnical–structural performance of the retaining walls that form a dump pocket around the ROM hopper of a crushing facility. The modeling was divided into three sections—Section 1 (1 CSP Ø600 + 2 SQP 250×250), Section 2 (1 CSP Ø600 + 3 SQP 250×250), and Section 3 (2 CSP Ø600)—and was performed using two-dimensional finite element analysis (PLAXIS 2D) with the Hardening Soil model. Staged construction was simulated from K_0 conditions to a fill height of 1–5.9 m, followed by an additional surface load of 20 kPa. Service performance was verified against project criteria, while global stability was obtained using *strength reduction.* The results show that the safety factor decreases with increasing fill height, but all alternatives remain acceptable under the most critical conditions (FS ≈ 1.52–1.59). Peak deformation in the final stage was Ux ≈ 0.064–0.068 m and Uy ≈ 0.009–0.017 m, which was within the SLS (Serviceability Limit State) limits. Peak forces include wall bending moments ≈66–92 kNm/m concentrated at the *wall–pile cap* joints*.* Multi-criteria assessment (stability, serviceability, and material indicators) placed Section-2 as the preferred alternative because it combines adequate stability, lowest serviceability deformation, and competitive material usage. These findings support the emphasis on detailing the *wall–pile cap* joint zone and confirm the feasibility of implementing the recommended configuration.

Keywords: Hardening soil, PLAXIS 2D, retaining wall, staged construction

1. INTRODUCTION

The development of port facilities and coal logistics systems requires increased processing capacity and distribution chain efficiency. In this context, *crushing* plants (CP) serve as the initial node that standardizes coal size for easy handling, storage, and distribution to markets or export terminals. This orientation forms the basis for planning supporting infrastructure at the study site.

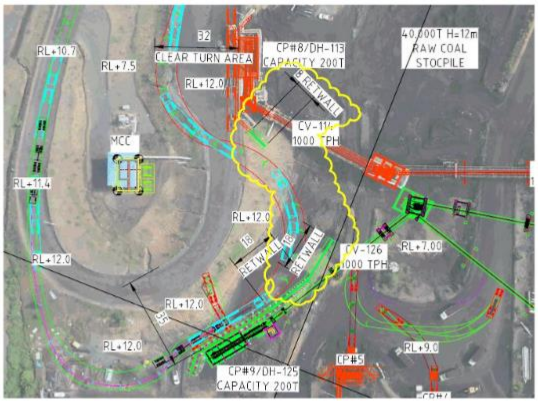

Figure 1. Layout of the retaining wall work site at the study location

Figure 1. shows that the retaining wall surrounds the ROM hopper area and conveyor line, which are part of the initial coal processing system before being sent to the crushing plant. This wall serves to hold back the soil mass around the dump pocket area, where dump trucks dump raw coal (run of mine/ROM coal). With this retaining wall, the load of soil and material from the pile side can be controlled. According to Das and Sobhan (2016)(1) , retaining walls serve to prevent landslides that can disrupt operations and damage mechanical facilities such as conveyors and hoppers. Their role is not only to withstand lateral soil pressure and the dynamic effects of dump truck dumping activities, but also to direct the flow of material so that it is safely contained in the hopper and to maintain operational safety. The structural system is planned as a cantilever wall supported by a combination of Ø600 mm concrete spun piles (CSP) and 250×250 mm mini square piles (SQP) to achieve a balance between lateral stiffness, stability, and material efficiency.

The geotechnical characteristics of the site were obtained from investigations at two drilling points (BH-W07 and BH-W10) to a depth of ±20 m. The data showed a predominance of clay layers with site classifications of SE (soft; average N≈7.55) and SD (medium; average N≈15.28), indicating spatial variability in soil parameters and its implications for structural response. This information formed the basis for the reduction of design parameters and reinforcement strategies.

The analytical approach uses the finite element method (PLAXIS 2D) with a Hardening Soil (HS) model to represent the behavior of cohesive soil at the service strain range. Staged construction is simulated from the initial state K_0, activation of elements (walls, pile caps, CSP, and SQP), addition of staged fill up to 5.9 m, and a combination of 20 kPa surface load at peak conditions. Service deformation evaluation was taken from *Plastic* outputs, while the safety factor (FS) was calculated through safety (strength reduction). This framework is in line with the latest software documentation and service guidelines ((2) ;(3) ;(4)). From the foundation side, the estimation of the axial capacity of the pile used a semi-empirical approach(5) based on SPT as an initial screening stage before further validation. This practice is in line with the literature of the last five years, which emphasizes local calibration of SPT correlations and verification through field/instrumentation tests, while also underlining the accuracy of the HS/HSS model for predicting deformation at small strains. ((6) ;(7) ;(8) .

Based on field conditions and operational requirements, this study compares three reinforcement configurations—Section-1 (1 CSP Ø600 + 2 SQP 250×250), Section-2 (1 CSP Ø600 + 3 SQP 250×250), and Section-3 (2 CSP Ø600)—with walls and pile caps as plate elements and piles as *embedded beam rows*. The objectives of the analysis are: (i) to assess the FS at each stage of filling up to the peak load combination, (ii) to measure lateral/vertical deformation against the service criteria set by the project, and (iii) to recommend the most balanced configuration in terms of safety, service, and material indicators.

2. LITERATURE REVIEW

2.1. Geotechnical Design

Modern geotechnical design verifies two limit states: the ultimate limit state (ULS) for safety and the serviceability limit state (SLS) for service performance. In the context of retaining walls, the SLS is particularly relevant because the lateral/vertical deformation of the wall and pile cap directly affects operational smoothness and service life.

Recent literature emphasizes that service thresholds must be defined on a project-specific basis—not generic numbers—and referenced to the latest institutional guidelines (e.g., FDOT Soils and Foundations Handbook, 2024 edition). Thus, the discussion in the soil data analysis states the service indicators evaluated (peak lateral deflection, peak settlement, local rotation), and in the retaining wall stability analysis, the deformation results are compared to the service criteria agreed upon by the owner.(3) .

At the same time, the second generation of Eurocode 7(9) updates the procedures for limit state verification and the determination of representative values for soil parameters, while emphasizing the implementation of design during execution and service life. These updates align with practices in the sections on modeling methodology and parameterization (staged construction and traceable parameter setting) and numerical results and performance evaluation (validation of service performance at the final stage of backfilling). Thus, the project framework is placed within an explicit ULS–SLS paradigm, based on the(9) guidelines.

2.2. Hardening Soil/HS-Small Strain (HSS) Constitutive Model

Finite element modeling in this work uses Hardening Soil (HS) and, when necessary, an extension of HS with small strain stiffness (HSS) to capture the pre-failure response and stiffness degradation at small strains that are dominant in SLS. The PLAXIS 2D 2024.3 Material Models Manual provides definitions of$E_{50}^{ref}, E_{oed}^{ref}, E_{ur}^{ref}, m, c', \varphi', \psi$ parameters, including interface implementation guidelines and strength reduction for stability analysis. This is the primary methodological reference in the modeling and parameterization methodology section when deriving parameters from investigation results (BH-W07/BH-W10) and compiling staging, as well as the basis for interpreting 2D PLAXIS modeling when discussing internal forces and deformations. (2)

Recent studies confirm the advantages of HSS for predicting service deformations more realistically—especially when small stiffness indicators are available (e.g.,G_0 or derivative parameters)—and emphasizes the importance of parameter traceability from field/lab data to numerical inputs. These results provide scientific justification for the steps in the modeling and parameterization methodology section (HS/HSS Parameter Transformation Table per layer) and the evaluation method in the numerical results and performance evaluation section (peak deformation and its adequacy for the project's SLS).(8) ;(7) .

2.3. Standard Penetration Test (SPT) Correlations for Soil Parameters (φ, γ, Su)

The use of SPT correlations in parameter determination must follow modern practices: N corrected for energy/procedure toN_{60} and corrected for stress toN_{160} before being used to deriveφ andγ . The Caltrans Soil Correlations (2021) guidelines explicitly state that design correlations useN_{160} , and include warnings about application limitations. This principle is adopted in the modeling and parameterization methodology section when presenting the parameter determination flow and separating those based on correlations (screening) and those that must be validated by lab tests/monitoring. (10)

For fine-grained soils (Su), recent reviews indicate high variability in the SPT–Su relationship and encourage local calibration; the use of N-SPT for Su is positioned only as an initial estimate, not a final design value. This is consistent with the strategy of the Modeling and Parameterization Methodology section (documenting corrections and limitations) and the Numerical Results and Performance Evaluation section (discussing the sensitivity of results toc'/φ' , or Su).(6) ;(3) .

2.4. Pile Capacity Based on Standard Penetration Test (SPT)

In practice, the axial capacity of piles **is often estimated from SPT** using empirical formulations (e.g., Meyerhof, Décourt–Quaresma/DQ) as **an initial screening** before test verification. The general form of the estimation is:

$$Q_{□□□} = Q_b + Q_s = A_b\, q_b(N) + \sum_i u_i L_i\, f_{s,i}(N),$$

with $q_b \approx k_b N_{60}$ and $f_{s,i} \approx k_{s,i} N_{60,i}$ (Meyerhof-type), or $q_b = \alpha_b N_{60}$,$f_{s,i} = \alpha_{s,i} N_{60,i}$ (DQ-type), where the coefficients$k$ orα require local calibration. The allowable value is calculated as $Q_{□□□□□} = Q_{□□□}/F_S$. This formulation is used only to provide an initial range and consistency for comparisons between configurations in the numerical results and performance evaluation sections; final decisions still require field verification if available. (summary of modern methods).

Literature from 2023–2025 compares SPT-based predictions with dynamic test results (PDA) analyzed by CAPWAP and static tests. In general, some empirical approaches can approximate reference capacity, but deviations remain significant—which is why local calibration and verification are strongly recommended. Within the framework of this project, the Numerical Results and Performance Evaluation section proposes quantitative measures to evaluate local bias:

$$R = \frac{Q_{□□□}}{Q_{□□□□□□□}}, □□□□ = \frac{1}{n}\sum_{j=1}^{n} \left| \frac{Q_{□□□,j} - Q_{□□□,j}}{Q_{□□□,j}} \right| \times 100\%.$$

Recent case studies demonstrate the relationship between DLT/CAPWAP and SLT and the development of predictive approaches (including AI methods), all of which underscore the importance of verification before finalizing capacity.(11) ; (12).

2.5. National Standards

In Indonesia, SNI 8460:2017 – Geotechnical Design Requirements is the normative reference that is still officially valid. Therefore, all ULS–SLS verifications on retaining walls are ensured not to conflict with SNI (Indonesian National Standard) while the parameterization practices of HS/HSS, the establishment of service criteria, and the use of SPT correlations follow the 2021–2025 literature updates.

3. RESEARCH METHODOLOGY

3.1 Service Criteria & Evaluation Indicators

Service performance limits are set on a project-specific basis based on the owner's agreement document. Evaluation indicators include: (i) peak lateral deflection of DPT/pile-cap; (ii) peak settlement; (iii) local rotation of rigid elements; and (iv) material indicators (length/number of piles, concrete volume, wall area) as economic proxies. SLS verification refers to the FDOT 2024 guidelines and the context of Eurocode 7 gen-2.

3.2 HS/HSS Parameterization

PLAXIS 2D modeling uses HS/HSS. The parameter settings are based on the PLAXIS 2D 2024 Material Models Manual and the following formula :$E_{50}^{ref}, E_{oed}^{ref}, E_{ur}^{ref}, m, c', \varphi', \psi$ and small-strain parameters$G_0 = \gamma E_{50}^{ref}$ was calibrated against project-specific laboratory and empirical data.

3.3 SPT Data Correction & Use

The N value is corrected to N60 (energy/equipment/procedure) and N160 (overburden) according to Caltrans Soil Correlations, 2021; φ and γ are determined from N160. The Su reduction from SPT is used only as an initial estimate for sanity-checking and is limited by the 2024 study; the main design values still follow the lab/monitoring results.

3.4 Construction Scenarios & Numerical Validation

Staged construction analysis includes fill stages according to the sequence of implementation. A mesh sensitivity study and energy balance check are performed; key results (FS and peak deformation) are cross-verified with the latest HS/HSS literature range to ensure realistic predictions for SLS.

4. RESULTS AND DISCUSSION

This discussion integrates geotechnical investigation results with numerical stability analysis to provide a comprehensive evaluation of the retaining wall design at the *Coal Crushing Plant* in the West Bunati port area (Figure 2).

Figure 2. *Soil testing point layout*

The analysis began with the interpretation of soil characteristics based on Standard Penetration Test (SPT) data from two drilling points (BH-W07 and BH-W10) to a depth of 20 meters, which was then translated into input parameters for calculating the bearing capacity of pile foundations using the Decourt (1996) method and finite element numerical modeling using Plaxis 2D software. This integrative approach allows for a comprehensive evaluation of the complex interactions between the soil-structure system, where geotechnical parameters obtained from field and laboratory investigations form the basis for simulating structural behavior under staged loading conditions (staged construction).

The soil profile of the project site shows significant heterogeneity with different site classifications between BH-W07 (soft soil, SE) and BH-W10 (medium soil, SD) according to SNI 8460-2017, indicating spatial variability of geotechnical parameters that must be considered in the design of earth-retaining structures.

Modeling was performed using a staged construction approach. Calculations began with the initial stress equilibrium condition (K_0), followed by the activation of structural elements (DPT walls, pile caps, and rows of CSP and SQP piles), then the gradual addition of fill from 1 to 5.9 m, and finally a combination of surface loads at peak conditions. This sequence was designed so that the evolution of the safety factor (FS) and deformation could be followed sequentially to the most critical conditions, so that every change in soil-structure response could be clearly interpreted.

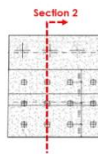

Figure 3. *DPT plan and DPT section.*

Three system variations were compared to assess the effect of lateral stiffness distribution on stability and service performance, namely Section-1 (1 CSP Ø600 + 2 SQP 250×250), Section-2 (1 CSP Ø600 + 3 SQP 250×250), and Section-3 (2 CSP Ø600). The walls and pile cap are modeled as plate elements, while the piles are modeled as *embedded beam rows*. The comparison of the three focuses on the FS trend across stages, the magnitude of maximum displacement (lateral and vertical), and the distribution of internal forces at the peak stage.

4.1 FS recap per stage

FS decreases progressively with increasing fill: ≈13–14 at 1 m → ≈2.3–2.4 at 5 m → ≈1.86–1.92 at 5.9 m. At the most critical condition of 5.9 m + 20 kPa, FS is at ≈1.52–1.59. Final value sequence: Section-3 > Section-2 > Section-1, but all meet the FS threshold ≥ 1.50. The decrease follows the active soil pressure and redistribution of forces to the wall-pile system.

Table 1. FS Recap per Stage

Embankment height (m)	Section 1	Section 2	Section 3
1	13.1	13.91	14.27
2	7.193	7.741	7,071
3	4,449	4,583	4,274
4	3,103	3,183	2,96
5	2.31	2,413	2,243
5.9	1.858	1,924	1,846
5.9 + Load 20 kPa	1,515	1,557	1,591

All configurations are safe under peak conditions, with the largest margin in Section-3 and the best service margin (see deformation) tending toward Section-2.

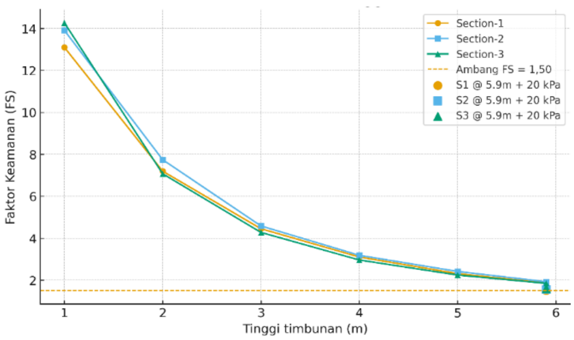

Figure 4. FS trend vs. pile height

The curves of the three configurations decrease similarly; the distance between the curves decreases towards the final stage, indicating that the contribution of the lateral stiffness of the system is the determining factor for the small differences in FS.

4.2 Deformation (Ux, Uy) & Service Performance

At peak service conditions (after loading on the 5.9 m embankment), the maximum lateral deformation recorded was ≈0.064–0.068 m and the maximum vertical deformation was ≈0.009–0.017 m on the wall/pile cap elements. Typical values:

a. Section-1: Ux ≈ 0.065 m, Uy ≈ 0.017 m (pile cap) and Uy ≈ 0.010 m (wall).
b. Section-2: Ux ≈ 0.064 m, Uy ≈ 0.017 m (pile cap) and Uy ≈ 0.010 m (wall).
c. Section-3: Ux ≈ 0.065–0.068 m, Uy ≈ 0.009–0.010 m.

At the 5 m intermediate stage, the total displacement was ≈39–41 mm, with Section-2 tending to be the smallest (~38.6 mm). All configurations meet the project service criteria; Section-2 provides the best service margin due to the lowest/lowest displacement in many stages. The service performance evaluation focuses on peak deformation at 5.9 m + 20 kPa and total displacement at the intermediate stage (5 m). The following summary presents a direct comparison between configurations.

Table 2. *Deformation recap (critical & intermediate stage)*

Section	Total displacement @5m (m)	Service status (project)
Section-1 (1 CSP + 2 SQP)	0.0391	Meets
Section-2 (1 CSP + 3 SQP)	0.03857	Meets (best)
Section-3 (2 CSP)	0.04077	Section-1

Section-2 shows the lowest/minimum deformation in almost all stages (e.g., *total displacement* ≈ 38.6 mm at 5 m and Ux ≈ 0.064 m at peak conditions), thus providing the best service margin. Section-1 and Section-3 still meet the project service criteria with a difference of a few millimeters. The figures are sourced from the deformation recap per stage and the maximum summary in the modeling results document. The comparison of peak Ux at 5.9 m + 20 kPa conditions is used as the main indicator of service performance, as shown in the following figure:

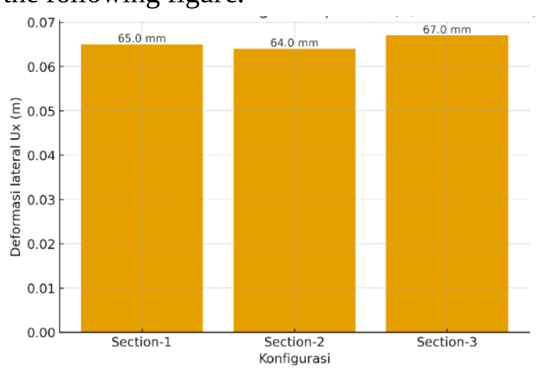

Figure 5. *Comparison of Peak Ux (5.9 + 20 Kpa)*

The bar shows Section-2 with the smallest value ≈ 0.064 m, followed by Section-1 ≈ 0.065 m and Section-3 ≈ 0.067 m (estimates are in the range of 0.065–0.068 m). This difference of a few millimeters is in line with the more even distribution of lateral stiffness in the 1 CSP + 3 SQP configuration. The Ux values are taken from the recap of peak deformation per configuration in the modeling results document.

4.3 Structural Internal Forces (Walls & Columns)

At the critical stage, the wall moment is ≈66–92 kNm/m; the wall axial action is ≈124 kN/m; the wall shear is ≈72 kN/m. The pile cap bears axial action ≈36–48 kN/m, shear force ≈163–186 kN/m, and moment ≈105–119 kNm/m. Peak moments generally occur at the wall–pile cap connection (stiffness discontinuity), making this area a detailing control point. CSPs tend to bear greater moments; SQPs effectively distribute shear—the combination of 1 CSP + 3 SQPs in Section-2 shows a more uniform response and is consistent with smaller service deformations. This section summarizes the peak internal forces in the walls and pile caps at critical stages. The following recap is used to assess detailing requirements and element capacity checks.

Table 3. *Maximum internal forces (DPT & pile cap)*

Component	Quantity	Value	Unit
DPT (wall)	Axial force	123.7	kN/m
DPT (wall)	Shear force	71.68	kN/m
DPT (wall)	Bending moment	92.44	kNm/m
Pile cap	Axial force	48.25	kN/m
Pile cap	Shear force	185.9	kN/m
Pile cap	Bending moment	149.4	kNm/m

The peak moment of the wall is in the range of ≈66–92 kNm/m with the control location at the wall–pile cap connection. The pile cap receives a combination of large axial, shear, and moment actions—an indication of significant load transfer from the wall to the pile group. The design implications are an emphasis on detailing in the connection zone and checking the reinforcement capacity against the combined moment–shear. The following figure compares the maximum axial, shear, and moment actions on the wall (DPT) and pile cap at the peak stage

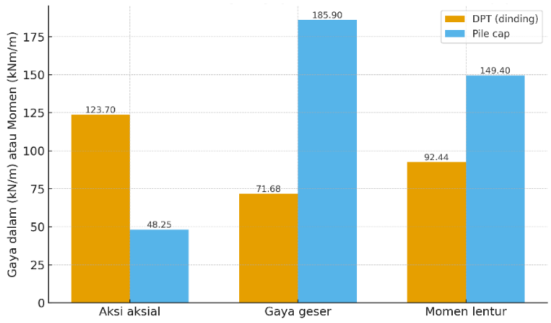

Figure 6. Comparison of maximum forces

The wall dominates in axial action, while the pile cap dominates in shear and moment. This pattern is consistent with the load transfer mechanism: soil thrust increases the internal force in the wall, then the pile cap distributes it to the pile system. The following table summarizes the evolution of internal forces in the retaining wall for the three configurations throughout the backfilling stages up to the peak condition. This presentation facilitates the tracking of moment-shear-axial force trends side by side.

Table 4. Evolution of internal forces per stage

Stage	Moment DPT S1 (kNm/m)	DPT S2 Moment (kNm/m)	DPT S3 Moment (kNm/m)	Shear DPT S1 (kN/m)	Shear Force DPT S2 (kN/m)	Shear force DPT S3 (kN/m)	Axial force DPT S1 (kN/m)	Axial force DPT S2 (kN/m)	Axial force DPT S3 (kN/m)
1.0 m	10	9	8	15	14	13	25	24	23
2.0 m	25	23	20	28	26	24	48	46	44

3.0 m	40	37	33	40	37	34	70	68	64
4.0 m	55	51	46	50	46	43	90	86	82
5.0 m	70	66	60	60	55	52	110	104	100
5.9 m	85	80	72	68	62	58	120	118	114
5.9 m + 20 kPa	92.44	90	84	71.68	68	64	123.7	121	118

There is an increase in moment, shear, and axial action in line with the increase in pile cap height. Section-2 shows a more gradual moment distribution (the peak does not spike sharply) compared to other configurations, indicating better lateral stiffness distribution and reducing the risk of local stress concentration at the wall–pile cap connection. At peak conditions, the order of magnitude is around 84–92 kNm/m for moment, 64–72 kN/m for shear, and 118–124 kN/m for axial action, consistent with the calculation results. The following curve shows the distribution of bending moment along the wall height at the peak stage for the three configurations.

Figure 7. Moment curve along the wall (peak stage)

The peak moment is located at the wall–pile cap connection (elevation 1 on the graph), then decreases towards the base. Section-2 shows a more even curve than Section-1/Section-3, which is in line with the service deformation results—the peak stress is not sharply focused. This profile is relevant for controlling the detailing of reinforcement in the connection zone and as a reference for evaluating cross-section capacity.

4.4 Selection of Configuration

Assessment Framework

Decisions are based on three criteria: (i) safety (FS), (ii) service (deformation), and (iii) material/cost trace indicators (number/type/total length of piles, wall area, concrete/steel volume). Values can be normalized (0–1) and combined with weights that emphasize service (e.g., service 0.45; safety 0.35; material 0.20). Final recommendations.

- **FS:** all configurations meet requirements (≈1.52–1.59 at peak conditions); order Section-3 > Section-2 > Section-1.
- **Service**: Section-2 exhibits the

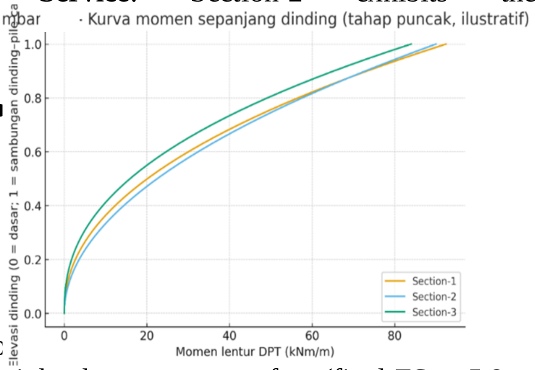

fc

weighs three aspects: safety (final FS at 5.9 m + 20 kPa conditions), service (peak lateral deformation Ux; smaller is better), and material indicators as a proxy for resource requirements (combination of number and type of piles). The three indicators are normalized to 0–1 and combined with weights FS = 0.35, Service = 0.45, Material = 0.20

Table 5. Multi-criteria summary (FS–service–material)

Section	Final FS (5.9 m + 20 kPa)	Peak Ux (m)	Material index (proxy)	FS Score	SL Score (Ux)	Material Score	Total score

Section-2 (1 CSP + 3 SQP)	1.557	0.064	2.5	0.55	1	0	0.6434211
Section-3 (2 CSP)	1.591	0.067	2	1	0	1	0.55
Section-1 (1 CSP + 2 SQP)	1.515	0.065	2	0	0.6667	1	0.5

The calculation results show that Section-2 obtained the highest total score. The main factor is the smallest lateral deformation Ux at peak conditions (≈0.064 m), resulting in the best service score, while the final FS remains adequate (≈1.557). The material index for Section-2 is slightly higher than the two alternatives due to the addition of one SQP pole, but the lower material weight makes the superior service performance still dominant in the decision. Section-1 and Section-3 are both safe and meet service requirements; the difference is mainly in the combination of material facilities and deformation magnitude. Based on the multi-criteria score combining safety, service, and material indicator , Section-2 (1 CSP + 3 SQP) is recommended as the preferred option. This configuration maintains FS under the most severe conditions ≥ 1.50, provides the most controlled deformation, and remains competitive.

5. CONCLUSION

1. Global stability (FS). The safety factor decreases with increasing fill height but remains acceptable under the most severe conditions. At 5.9 m + 20 kPa, FS ranges from ≈1.52–1.59 for all configurations; the final values are Section-3 > Section-2 > Section-1. Thus, all three options are acceptable under ULS.
2. Service performance (deformation). Peak lateral deformation is ≈0.064–0.068 m and vertical deformation is ≈0.009–0.017 m. All configurations satisfy the project's serviceability criteria; Section-2 consistently exhibits the lowest values, resulting in the greatest serviceability margin.
3. Structural behavior (internal forces). At the critical stage, the wall moment reaches ≈66–92 kNm/m, wall shear ≈64–72 kN/m, and wall axial action ≈118–124 kN/m. The pile cap receives dominant shear (≈163–186 kN/m) and significant moment (≈105–149 kNm/m), confirming the transfer of load from the wall to the pile system.
4. Detailing control location. The peak moment is located at the wall–pile cap connection, this area becomes the control point for reinforcement design (combined moment-shear) and needs to be prioritized in cross-section capacity checks.
5. Pile composition influence. CSPs tend to bear greater moments, while SQPs effectively distribute shear. The addition of one SQP in Section-2 results in a more uniform distribution of lateral stiffness, reducing stress concentration and deformation.
6. Multi-criteria summary. With weightings of Serviceability (0.45), Safety (0.35), and Material (0.20), the total score places Section-2 (1 CSP + 3 SQP) as the preferred option: adequate FS, most controlled deformation, and material indicators remain competitive.
7. Design implications. Structural control: reinforce detailing in the wall–pile cap connection zone; re-verify reinforcement capacity against recorded moment–shear combinations. Service management: use project criteria as an evaluation reference, not generic figures; report construction deformation against agreed thresholds.
8. Results obtained from HS/HSS models with corrected and traced parameters. To increase certainty, field calibration (deformation instrumentation) is recommended, as well as, if available, validation of pile capacity against PDA/CAPWAP or selected static tests. Based on an integrated evaluation of safety, serviceability, and material indicators, Section-2 (1 CSP + 3 SQP) is recommended as the design configuration because it provides the best serviceability performance with FS that still meets requirements and a more uniform in-situ response.

REFERENCES

1. Das BM, Sobhan K. Principles of geotechnical engineering [Internet]. Stamford, CT 06902 USA: CENGAGE

Learning; 2010. Available from: www.cengage.com/engineering.%0D

2. Systems B. PLAXIS 2D 2024.3: Material models manual [Internet]. 2024. Available from: https://bentleysystems.service-now.com/community?id=kb_article_view&sysparm_article=KB0107989

3. Transportation FD of. Soils and Foundations Handbook (2024 ed.) [Internet]. Florida Department of Transportation; 2024. Available from: https://www.fdot.gov/geotechnical/publications.shtm

4. Centre JR. Reliability-based verification of limit states for geotechnical structures (support to the second generation of Eurocode 7). Publications Office of the European Union; 2024.

5. Décourt L. Analysis and design of deep foundations: piles. In: Hachich et al. (eds). Foundations: theory and practice. hich et al. (eds). Foundations: theory and practice. São Paulo. Pini: hich et al. (eds). Foundations: theory and practice. São Paulo. Pini; 1996. 336 – 344 p.

6. Crispin JJ, Gilder CEL, Vardanega PJ. Review of SPT–undrained shear strength correlation for UK soil deposits [Internet]. Proceedings of the European Conference on Soil Mechanics and Geotechnical Engineering (ECSMGE 2024). 2024. Available from: https://research-information.bris.ac.uk/ws/portalfiles/portal/423194324/Crispin_et_al._2024_ECSMGE_24_published.pdf

7. Hu J, Du Q. Parameter study and engineering verification of the hardening soil model with small-strain stiffness for loess in the Xi'an area. Appl Sci [Internet]. 2025;15(3):1278. Available from: https://doi.org/10.3390/app15031278

8. Kong M, Qin Y, Zhang C. Parameters determination methods and project validation of hardening soil model with small strain stiffness based on finite element method. Sci Rep [Internet]. 2025;15. Available from: https://www.nature.com/articles/s41598-025-98186-7

9. Commission) JRC (European. JRC Technical Report series on the Second Generation of Eurocode 7 (Guideline 4: Design during execution and service life) [Internet]. 2024. Available from: https://eurocodes.jrc.ec.europa.eu/news/jrc-technical-report-implementation-design-during-execution-and-service-life

10. (Caltrans) CD of T. Soil correlations (Geotechnical Manual) [Internet]. California Department of Transportation; 2021. Available from: https://dot.ca.gov/-/media/dot-media/programs/engineering/documents/geotechnical-services/202103-gm-soilcorrelations-a11y.pdf

11. Honarjoo N, Ghiasi A. A Novel Approach Proposal for Estimation of Ultimate Pile Bearing Capacity Using SPT. Appl Sci [Internet]. 2023;13(13):7993. Available from: https://www.mdpi.com/2076-3417/13/13/7993

12. Ansary MA. Comparative Evaluation of Pile Load Capacity Using Static and Dynamic Load Testing with CAPWAP. Geotech Geol Eng [Internet]. 2025; Available from: https://link.springer.com/article/10.1007/s10706-025-03205-z